Comparison of chemisorption close to ambient vs. under reaction conditions for Group VIII metal catalysts

Yu-Tung Tsai, James G. Goodwin Jr. *

Department of Chemical and Biomolecular Engineering, Clemson University, Clemson, SC 29634, USA

ABSTRACT

A comparison of the relationship of H_2 or CO chemisorption measurements at 25–100 °C to similar results obtained under CO hydrogenation conditions by steady-state isotopic transient kinetic analysis (SSITKA) is made for the first time for a wide variety of Group VIII metal catalysts. The ratio N_T^*/N_{chem} (amount of chemisorption by SSITKA vs. by static chemisorptions) was found to be almost always ca. unity for Co catalysts. SSITKA can, thus, be used as a complementary characterization technique to TEM, XRD, and static chemisorption for better understanding of Co metal catalyst dispersion and metal surface site availability for Co catalysts with a wide variety of promoters/supports. Unfortunately, application of SSITKA chemisorption measurements under reaction conditions for characterizing metal dispersion for the other metals is limited at this time. However, the results do suggest some possibilities for Ru and Rh.

© 2011 Elsevier Inc. All rights reserved.

1. Introduction

Metal catalysts comprised Co, Fe, Ru, Rh, Ni, or Pt are widely used in industrial applications. All are active to some degree for CO hydrogenation. The first five are also promising candidates for the production of alternative fuels by Fischer–Tropsch synthesis (FTS) [1–6]. Although much research has been undertaken in the past addressing their catalytic properties, the relationships of their metal surface structures to those properties are still not completely understood since measures of their adsorptive properties (used often to estimate metal surface areas, active site densities, and other surface properties) vary greatly with composition, conditions, and even the analysis method used.

H_2 or CO static chemisorption is used typically to estimate the number of surface metal atoms for most heterogeneous Group VIII metal catalysts [7–9]. Investigations have confirmed that such things as metal loading, nature of support, and the preparation method impact the stoichiometries for H_2 and CO adsorption on these metal catalysts. For example, Reuel and Bartholomew [10], in a systematic study of CO and H_2 adsorption on Co catalysts, showed that hydrogen adsorption is highly activated on cobalt,

with the degree of activation dependent on the metal loading. In addition, other complications that may affect chemisorption data analysis on various metals are suppression of H_2 chemisorption, formation of carbides, H_2 spillover, carbon deposition, the strong interaction between metal and supports (SMSI), the nature of chemisorption at metal–support interfaces, and the presence of promoters/poisons (illustrated in Fig. 1) [5,10–13]. Although the number of surface metal atoms and metal dispersion measured by chemisorption has been demonstrated to be related to the catalytic properties for many heterogeneous metal catalysts, the accuracy of such measurements is complicated by some of the problems mentioned above which limit the usefulness of these estimations.

Steady-state isotopic transient kinetic analysis (SSITKA) is one of the most powerful tools to estimate the surface residence time, concentration of intermediates, intrinsic site activities, and surface reaction mechanism under reaction conditions. It has been widely applied since the early pioneering work of Happel, Bennett, Biloen and Bell [14–17]. SSITKA provides in-situ surface kinetic information based on tracing the isotopically labeled effluent species vs. time after switching the flow of a reactant in the reactor feed labeled with one isotope to that labeled with another. Reactant and product concentrations are not disturbed by the isotopic switch (for elements heavier than hydrogen) under isothermal
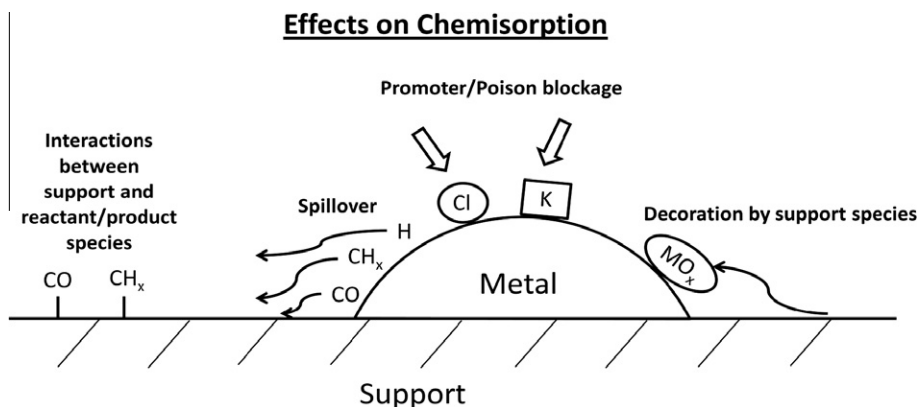
Effects on Chemisorption

Fig. 1. Factors that can affect surface coverage.

and isobaric reaction conditions. SSITKA allows determination of the surface concentrations of the most active reaction intermediates and reversibly adsorbed reactants, which provides an alternative way to obtain valuable information about chemisorption properties, especially at reaction conditions.

Significant transformations during reaction can affect not only the catalyst surface layer but also deeper structures by the formation of new microstructures or defects, which may be stabilized by various promoters. Such changes may only occur during reaction and may not exist during static chemisorption. In addition, rarely if ever, is the number of active sites on a catalyst equal to more than a small fraction of the number of available surface metal atoms, determined by static chemisorption [18]. Therefore, the estimation of active sites is more exact using SSITKA measurements. The surface concentration of CH_4 intermediates (N_M) is related to the number of reaction sites producing methane.

N_M, because it relates to the number of actual reaction intermediates, can be used to calculate a more true value of the TOF than that normally calculated using chemisorption. However, in this paper, since our interest is on comparing chemisorption at room temperature vs. reaction temperature, we will focus on N_T, the total concentration of adsorption species on the surface. The total amounts of chemisorption species under reaction (methanation) conditions (N_T) are the sum of N_M plus the surface concentration of CO reversibly adsorbing and desorbing (N_{CO}). It should be noted that SSITKA is performed at steady-state reaction conditions. However, static chemisorption is carried out usually for a metal catalyst after preparation and reduction. Therefore, one should keep in mind that the results from SSITKA measurements are after reaching steady-state reaction conditions, while the results for static chemisorption are for the catalyst in an initial state at 25–100 °C. This difference could affect the relationship between the chemisorption results for SSITKA and for static chemisorption.

The purpose of this study was to compare a wide variety of results based on static chemisorption and SSITKA techniques for chemisorption uptakes close to room temperature (RT $\sim$ 100 °C) vs. at reaction temperatures, respectively. Use was made of results from the literature for Group VIII metal catalysts employed for CO hydrogenation where both adequate static chemisorption and SSITKA data were reported. The relationship of the results at static chemisorption and reaction conditions are completely discussed. It is shown how the use of SSITKA as a complementary characterization technique to static chemisorption, XRD, and TEM for Co catalysts can help in determining the availability of metal surface atoms in cases where SMSI, promoters, poisons, and surface blockage by carbon deposition may skew understanding.

2. Methodology

2.1. Catalysts

Although static chemisorption and SSITKA have been widely applied in methanation studies for Group VIII catalysts, their measurements can only be compared when the data from both techniques are available in a given study. Many previous reports would be appropriate to be listed in this study but for the lack of comparable data, due to missing static chemisorption data [6,19–22], different conditions for reaction and SSITKA measurements [23], an isotopic transient method being used that is somewhat different from SSITKA [24] or because of a different isotope being traced [25]. Surprisingly, Ni catalysts are not able to be discussed in this paper because of insufficient comparable data [6,21,25]. A list of Co, Fe, Ru, Rh, and Pt catalyst studies in the literature containing sufficient chemisorption and SSITKA results for comparison is given in Table 1. All papers listed in Table 1 reported SSITKA studies under CO hydrogenation conditions and also provided H_2 and/or CO static chemisorption data. As shown in Table 1, the catalysts compared here utilized various supports (Al_2O_3, TiO_2, SiO_2, MCM-41, and carbon) and were often promoted with such species as Zr, Re, La, Ru, Cu, Mn, V, or alkali. Most catalysts were prepared by incipient wetness impregnation except for the Fe catalysts, which were prepared by a pH precipitation method.

2.2. SSITKA measurement during methanation

The FTS catalysts are usually investigated by SSITKA under methanation conditions (high H_2/CO ratios) due to simplicity of product analysis and less deactivation with TOS (time-on-stream). Methanation on Co, Ru, Fe, Rh, and Pt catalysts has been extensively studied by SSITKA [1–5,11–13,26–39].

SSITKA systems utilized to carry out reaction and isotopic analyses typically consist of a plug flow reactor (PFR) using small amounts of catalysts under differential conditions (i.e., for conversions often lower than 5–10%) to minimize the effects of heat and mass transfer and to simplify kinetic analysis. No significant readsorption occurs for methanation, suggesting that there is no effect of conversion, provided it is kept in the differential range. The general procedure for isotopic transient measurements of methane and CO during reaction involves a switch between input flows of ^{12}CO/Ar and ^{13}CO without disturbing the stability of the reaction. The purpose of adding a trace of Ar (5%) to CO is to determine the gas phase holdup time innate to the experimental system. The pressure on both feed streams is maintained by back-pressure regulators to a constant value in order to minimize disturbances

Table 1
Catalyst compositions and nomenclature.

Catalyst nomenclature for this paper	Original nomenclature	Primary metal (wt%)	Additive	Support	Reference
Co1	Co/Al	Co(20)	–	Al_2O_3	[30]
Co2	Co/Al–Zr-11	Co(20)	ZrO_2: 10.8 wt%	Al_2O_3	"
Co3	$12Co/\gamma$-Al_2O_3	Co(12)	–	γ-Al_2O_3	[31]
Co4	$12Co0.5Re/\gamma$-Al_2O_3	Co(12)	Re: 0.5 wt%	γ-Al_2O_3	"
Co5	$20Co0.5Re/\gamma$-Al_2O_3	Co(20)	Re: 0.5 wt%	γ-Al_2O_3	"
Co6	$20Co0.5Re/\alpha$-Al_2O_3	Co(20)	Re: 0.5 wt%	α-Al_2O_3	"
Co7	$12Co/TiO_2$	Co(12)	–	TiO_2	"
Co8	$12Co0.5Re/TiO_2$	Co(12)	Re: 0.5 wt%	TiO_2	"
Co9	$12Co/SiO_2$	Co(12)	–	SiO_2	"
Co10	$12Co0.5Re/SiO_2$	Co(12)	Re: 0.5 wt%	SiO_2	"
Co11	B-La0	Co(20)	La/Co = 0 (atomic ratio)	SiO_2	[1]
Co12	B-La10	Co(20)	La/Co = 0.1	SiO_2	"
Co13	B-La30	Co(20)	La/Co = 0.3	SiO_2	"
Co14	B-La75	Co(20)	La/Co = 0.75	SiO_2	"
Co15 [a]	Ru-promoted Co/Al_2O_3	Co(20)	Ru: 0.5 wt%	γ-Al_2O_3	[2]
Co16 [a]	"	Co(20)	Ru: 0.5 wt%	γ-Al_2O_3	"
Co17 [a]	"	Co(20)	Ru: 0.5 wt%	γ-Al_2O_3	"
Co18	5CoRu/M1	Co(5)	Ru: 0.5 wt%	MCM-41[b]	[36]
Co19	8CoRu/M1	Co(8)	Ru: 0.5 wt%	MCM-41[b]	"
Co20	14CoRu/M1	Co(14)	Ru: 0.5 wt%	MCM-41[b]	"
Co21	14CoRu/M2	Co(14)	Ru: 0.5 wt%	MCM-41[c]	"
Co22	14CoRu/S	Co(14)	Ru: 0.5 wt%	SiO_2	"
Co23	5CoRu/S	Co(5)	Ru: 0.5 wt%	SiO_2	[5]
Co24	$Co/Ru/TiO_2$	Co(12.04)	Ru: 0.18 wt%	TiO_2	[26]
Co25	Co/SiO_2	Co(23)	–	SiO_2	[27]
Co26	Co/Al	Co(20)	–	γ-Al_2O_3	[28]
Co27	Co/Ru/Al	Co(20)	Ru: 0.5 wt%	γ-Al_2O_3	"
Fe1	P9	Fe(20)	Cu: 5 wt%, K: 4.2 wt%	SiO_2	[33]
Fe2	100Fe	Fe(100)	–	–	[4]
Fe3	95Fe5Cr	Fe(95)	Cr: 5 wt%	–	"
Fe4	80Fe20Mn	Fe(80)	Mn: 20wt%	–	"
Fe5	90Fe10Zr	Fe(90)	Zr: 10wt%	–	"
Fe6	100Fe2.5 K	–	K/Fe = 0.015 (atomic ratio)	–	[3]
Fe7	FeMn	–	Mn/Fe = 0.20	–	"
Fe8	FeMn4 K	–	Mn/Fe = 0.20, K/FeMn = 4	–	"
Fe9	10 wt%Fe/γ-Al_2O_3	Fe(10)	–	γ-Al_2O_3	[32]
Ru1	RuSCu00	Ru(3)	Cu/Ru = 0 (atomic ratio)	SiO_2	[11,34]
Ru2	RuSCu05	Ru(3)	Cu/Ru = 0.05	SiO_2	[34]
Ru3	RuSCu10	Ru(3)	Cu/Ru = 0.10	SiO_2	"
Ru4	RuSCu20	Ru(3)	Cu/Ru = 0.20	SiO_2	"
Ru5	RuSCu50	Ru(3)	Cu/Ru = 0.50	SiO_2	"
Pt1	K Pt.0	Pt(4.5)	K^+/Pt = 0.1(atomic ratio)	SiO_2	[35]
Pt2	K Pt.1	Pt(4.5)	K^+/Pt = 0.2	SiO_2	"
Pt3	00K/Pt	Pt(20)	K^+/Pt = 0	C	[12]
Pt4	20K/Pt	Pt(20)	K^+/Pt = 0.2	C	"
Pt5	40K/Pt	Pt(20)	K^+/Pt = 0.4	C	"
Pt6	80K/Pt	Pt(20)	K^+/Pt = 0.8	C	"
Rh1	Rh/SiO_2	Rh(1.5)	–	SiO_2	[13]
Rh2	$Rh/V/SiO_2$	Rh(1.5)	V: 1.5 wt%	SiO_2	"
Rh3	Rh/Al_2O_3	Rh(5.2)	–	γ-Al_2O_3	[37,38]
Rh4	Rh/MgO	Rh(2.5)	–	MgO	[39]

[a] Co15: calcined at 300 °C; Co16: calcined at 350 °C; Co17: calcined at 400 °C.
[b] MCM-41 with small pores.
[c] MCM-41 with large pores.

during switching of the feed streams. The effluent gas is monitored online by GC, for reaction rate and product distribution, and a mass spectrometer (MS) with a high-speed acquisition system for the isotopic transients. Information about the calculation of the surface residence times and the concentration of active surface intermediates has been given in detail elsewhere [18,29,40].

The methanation conditions applied in SSITKA are typically the same as for CO hydrogenation in general except that the ratio of H_2 to CO and the temperature are usually higher. This shifts the product distribution to CH_4 as the primary product, which simplifies the mass spectrometric (MS) online isotopic analysis during SSIT-KA. Table 2 summarizes the methanation conditions utilized by the studies discussed in this paper. Except for the Pt catalysts, most catalysts were investigated under a total pressure of 1.0–1.8 atm and for a temperature range of 180–300 °C, with a H_2/CO ratio of

2–20. Methanation on Pt was studied at 2.56 atm and 392 °C with H_2/CO = 20. Such a high temperature is required due to the low activity of Pt for CO hydrogenation.

2.3. Static chemisorption measurements at 25–100 °C

H_2 or CO static chemisorption was performed typically at 25 or 100 °C. The catalysts were generally reduced in a hydrogen flow at a specific temperature (usually the same as the reduction temperature applied in the reaction study) prior to chemisorption measurements. Particle sizes and active metal dispersion were calculated based on the assumption of a stoichiometry between chemisorbed gas molecules and surface metal atoms, typically 1:1 for both CO/M_s and H/M_s when M_s is a surface metal atom. The representative static chemisorption quantity used (total vs.

Table 2
Methanation conditions for SSITKA measurements on the catalysts reported in this paper.

FTS catalysts	Reaction temp. (°C)	Pressure (atm)	H$_2$/CO ratio	Reference
Co	202–225	1.18–1.82	2–15	[1,2,5,26–28,30,31,36]
Fe	265–280	1.00–1.80	9–20	[3,4,32,33]
Ru	240–270	1.80	5–20	[11,34]
Pt	392	2.56	12	[12,35]
Rh	180–300	1.00–1.80	9–20	[13,37–39]

irreversible) varied with different metals, depending on what has been established in the literature by the best correlation with physical techniques, such as TEM. For example, total chemisorption uptake is employed for the estimations of metal dispersion for Co, Fe, Pt, and Rh catalysts. Valid estimations for Ru catalysts, however, can only be obtained by using irreversible chemisorption uptake.

2.4. Nomenclature

The nomenclature for the static chemisorption and SSITKA parameters in this study is as follows. N_{CO}^* and N_M^* represent the concentration of adsorbed CO and methane intermediates, respectively, on the surface under reaction conditions as measured by SSITKA (identified by "*"). Note that the concentration of hydrogen atoms on the surface during reaction, unlike C-containing species, cannot be measured by SSITKA accurately due to the isotope effect. However, it is well known that during CO hydrogenation, most of the metal surface is covered by CO and CH$_x$ species since little free hydrogen exists in the presence of CO due to competitive adsorption by CO [10], although it is possible that for some catalyst systems or at very particular reaction conditions, this may not be true. N_T^* represents the total amount of species adsorbed on the surface in terms of carbon atoms from SSITKA measurements $(N_T^* = N_{CO}^* + N_M^*)$. N_H and N_{CO} give the amounts of uptake from static H$_2$ and CO chemisorption, respectively. N_{chem} is a general term for the uptake from chemisorption and can stand for either N_H or N_{CO} depending on whether H$_2$ or CO chemisorption was measured.

The nomenclature for the catalysts has been changed from the original references for an easier comparison in this paper. All catalysts are renamed in Table 1 in the form of "main metal + number". For example, Co1 represents a Co catalyst, the first in the list of Co-based catalysts, consisting of 20 wt% Co/Al$_2$O$_3$ which had an original nomenclature of Co/Al, reported in Ref. [30].

3. Results and discussion

3.1. General

The adsorption of CO and H$_2$ on several metal catalysts during CO hydrogenation has been widely investigated [41,42]. It was found that at FTS conditions, most hydrogen chemisorption is reversible. The rate of hydrogen desorption is relatively faster than the rate of hydrogen adsorption. Chemisorption of CO is much stronger than that of hydrogen at FTS conditions [10], and thus, the surface is primarily covered by CO and hydrocarbon intermediates, and the coverage by hydrogen is very low as indicated in the previous section.

Thermodynamics, kinetics of the given reaction, and reaction/chemisorption conditions determine whether the amount of chemisorbed species measured by static chemisorption is similar to that detected by SSITKA. Thus, it has to be anticipated that measurements could be different from static chemisorption for SSITKA of a particular reaction or at particular reaction conditions. Surface coverage of adsorbed species calculated from static chemisorption results could possibly be different from that determined by SSITKA

simply due to differences in the temperature of measurement. Several major factors affecting surface coverage on metals will be discussed later.

The ratio N_T^*/N_{chem} can be an indication of any such differences in the measurements. Before discussion of the results for the various metal catalysts, it is useful to list the possibilities for the ratio and the corresponding implications. These possibilities are as follows:

(a) $N_T^*/N_{chem} \approx 1$
When N_{chem} has a similar value as N_T^*, there is a good possibility that:
- There is full surface coverage for $T_{chem} - T_{SSITKA}$.
- $N_{chem} \approx N_T^* \approx \sum N_i^* \approx N_{metal,s}$
where $N_{metal,s}$ = the number of exposed surface metal atoms. A valid calculation of metal dispersion and particle size can be obtained from either N_T^* or N_{chem}, provided there is no decoration of the metal surface by support/promoter species.

(b) $N_T^*/N_{chem} > 1$

A significantly smaller value of N_{chem} than N_T^* for a specific metal catalyst would most likely indicate difficulty in getting full surface metal atom coverage during chemisorption measurements, probably due to the temperature of chemisorption being too low for adequate kinetics of adsorption, especially with the use of automated chemisorption systems. The effect is particularly evident for catalysts with low metal loadings, low reducibilities, or strong metal–support interactions which can affect the chemisorption kinetics [10,43].

Much previous literature has focused on the fact that chemisorption properties of Group VIII metals can be dramatically altered by reducible metal oxide supports, such as TiO$_2$ [9,44]. For example, the suppression of H$_2$ and CO chemisorption in metal/TiO$_2$ systems is typically caused by site blockage due to the TiO$_x$-overlayers formed during high-temperature reduction [45]. The dispersed metal particles may also agglomerate or sinter at higher reduction temperatures resulting in a decreased chemisorption [46], although this should be the case for both static chemisorption and SSITKA measurements, provided the same catalyst reduction temperature is used.

(c) $N_T^*/N_{chem} < 1$

When $N_{chem} > N_T^*$, there could be a number of possible reasons. The first relates to the phenomenon of H$_2$ spillover. The term spillover, in heterogeneous catalysis, is used to describe the transport of chemisorption species from the primary adsorption sites on one phase to those on another of the catalyst which essentially do not adsorb these species directly at the given conditions [47]. It is known that the contribution of H$_2$ spillover is hard to quantify and can be altered markedly in the presence of impurities, especially water and carbon-containing species [48]. H$_2$ spillover is more likely to happen at a higher H$_2$ pressure or a higher temperature. The simplest way to determine the existence of H$_2$ spillover is to calculate the hydrogen-to-metal surface atom ratio

($N_H/N_{metal,s}$), where $N_{metal,s}$ is determined by a physical method like TEM or XRD. The $N_H/N_{metal,s}$ ratio should be larger than unity when spillover occurs [49].

A second explanation for $N_{chem} > N_T^*$ could be the effect of chemisorption equilibrium resulting in lower surface coverage ($\theta < 1$) of adsorbed species at the higher temperature used for reaction.

A third possibility could be that the number of active sites of the catalyst is reduced by carbon deposition/coke formation under reaction conditions. Carbonaceous deposits may accumulate significantly (e.g., in the order of 15 wt% of the catalyst) and accordingly deactivate the catalyst either by blocking pores or by covering active reaction/adsorption sites [50,51]. For instance, Ni catalysts have been found to be very active for dry reforming of methane with CO_2 [52,53] and for direct cracking of methane to hydrogen [54]. However, Ni catalysts deactivate quickly due to coking. Mechanisms of carbon deposition and coke formation on metal catalysts have been studied extensively [55,56].

Finally, changes in the physical/chemical makeup of the catalyst could occur at reaction conditions resulting in a loss of active metal sites. Some changes include sintering and solid-state transformation. Sintering causes the loss of active surface via structural modification or coalescence of small metal crystalline into larger ones. Solid-state transformation at higher reaction temperatures results in the formation of different crystalline phases which may result in significant changes in chemisorption and catalytic activity. Experimental observations have shown that sintering and solid-state transformation rates of supported metal catalysts can be significantly affected by the temperature [50]. Obviously, some such changes could also occur during standard reduction in the catalyst. If so, the effect should be seen in both static chemisorption and SSITKA measurements.

(d) Other issues

There are two more points that need to be addressed before any comparison. Firstly, the N_T^*/N_{chem} ratio would be affected by the stoichiometry of adsorption for the active reaction intermediates. For example, the assumption of H/M_s or $CO/M_s = 1:1$ is typical for H_2/CO chemisorption. However, the active intermediate, CH_x or CO, measured by SSITKA at reaction temperature may not occupy a single metal surface atom as a site. If so, then the ratio of N_T^*/N_{chem} would not be unity (i.e., N_T^* having a value very similar to that of N_{chem}) even if the surface was to be completely covered with adsorbed species.

Secondly, the comparison attempted in this study is also valid only if the active reaction intermediates are formed/adsorbed only on the metal surface, which is true for the methanation reaction discussed in this study. If readsorption of reaction intermediates/ products can take place on non-metal sites, such readsorption must be accounted for before a comparison can be made [57,58]. If bifunctional catalysis takes place, a comparison with static chemisorption would not be correct.

3.2. Co catalysts

Table 3 gives the comparison of static chemisorption (H_2 chemisorption at 100 °C) and SSITKA (at reaction temperature) results for Co catalysts [1,2,5,26–28,30,31,36]. The ratio N_T^*/N_{chem} for all these Co catalysts varied between 0.61 and 1.83. Most of the catalysts had values that fluctuated within the smaller range of 0.9–1.1. In other words, for most Co catalysts, the value of N_T^*/N_{chem} was close to unity. Let us now address why all Co catalysts do not give such an ideal result. Higher ratios were observed for some specific supports. For example, suppression of H_2 chemisorption due probably to strong interaction of the metal with the support has been sug-

gested to explain the low hydrogen uptakes for TiO_2-and small pore MCM-41-supported Co catalysts (Co7–Co8 and Co18–Co20) [31,36]. TiO_2 is a well-studied support where strong metal support interaction has been observed [45,59]. The migration of partially reduced TiO_2 species onto the metal surface has been proposed to cause the suppression of chemisorption in part by a physical blockage of active surface sites. This suppression/blockage would seem to cause also a decrease in the surface concentration of intermediates measured by SSITKA since Ti^{3+} cations can be produced by reduction as low as 200 °C [45]. Therefore, ratios of N_T^*/N_{chem} having values of 1.2–1.3 for Co7 and Co8 are not surprising, although the reduction temperature was only 350 °C. The effect was even more significant for small pore MCM-41-supported catalysts (Co18, Co19, and Co20), giving values of N_T^*/N_{chem} of 1.36–1.83.

The values of N_T^*/N_{chem} for Co catalysts appear to be able to be decreased by specific promoters. For example, the value gradually decreased as the amount of La promotion increased (Co11–Co14) for La/Co = 0–0.75. However, the ratios still remained relatively close to unity (0.75–1.25).

Co15–17 and Co27 were all $Co/Ru/Al_2O_3$ with the same amounts of components (20 wt% Co and 0.5 wt% Ru). The effect of preparation could be a possible explanation for differences in the ratio seen because Co15–17 were calcined at 300, 350, and 400 °C, respectively, while Co27 was calcined at 300 °C. This might explain why Co15 had a closer value to Co27. The observed difference between these latter two catalysts may be explained by differences in reaction conditions (such as total flow rate).

3.3. Fe catalysts

A number of SSITKA studies have addressed for bulk Fe-based FTS catalysts (Table 4) [3,4,32,33]. It can be seen from Table 4 that values of N_T^* were only a small fraction of N_{chem} for most of the Fe catalysts. The N_T^*/N_{chem} ratios varied from 0.05–0.86. A possible explanation for the small N_T^* for Fe1 could be due to not including N_{CO}^* since it was not reported in the study [33]. However, this does not explain the results for Fe2–Fe9 where N_{CO}^* was reported. The small N_T^* amounts for Fe2–Fe9 may be explained by site blockage following carbon deposition (mainly in the form of inactive coke) at reaction temperature [3,4]. A larger N_T^*/N_{chem} could be observed for K-promoted Fe or FeMn catalysts (Fe6 and Fe8) compared to that for unpromoted ones (Fe2 and Fe7), suggesting that (1) K species may have covered part of surface Fe atoms which results in lower CO chemisorption and (2) the amount of carbon deposition in the form of χ-Fe_2C_5, which has been suggested to be the major Fe active carbide phase for FTS [60], increased with increasing K content. The presence of Fe-carbide appears to significantly increase N_T^* at reaction temperature.

3.4. Ru catalysts

Table 5 shows the results of two studies of Ru catalysts – one with only non-decorated Ru (Ru1) [11] and the other with Cu-decorated Ru catalysts (Ru2–Ru5) [34]. For the Ru catalyst without Cu decoration (Ru1), N_T^* remained pretty much constant with reaction temperature (in the range 240–270 °C) for a given H_2 partial pressure. A similar behavior could be observed also for the TOS study. N_T^*/N_{chem} ratios remained at about 2 (1.71–2.21) for Ru1, depending on P_{H_2} and P_{CO} during reaction. It is noted that N_M^* decreased with increasing H_2 partial pressure at a specific reaction temperature.

For Cu-decorated Ru catalysts (Ru2–Ru5), as can be seen from Table 5, Cu significantly blocked hydrogen chemisorption sites. H_2 chemisorption in Ref. [34] was carried out at −196 °C in order to estimate the number of Ru surface atoms and to exclude hydrogen

Table 3
Chemisorption and SSITKA (methanation) results for Co catalysts.

Catalyst samples	Support	Additive	N_{chem} (μmol H/g cat.)	N_{CO}^* [e] (μmol/g cat.)	N_M^* [e] (μmol/g cat.)	N_T^* [e] (μmol/g cat.)	N_T^*/N_{chem}	Reference
Co1	Al$_2$O$_3$	–	59[a]	39	10	49	0.83	[30]
Co2	Al$_2$O$_3$	ZrO$_2$: 10.8 wt%	64[a]	41	17	58	0.91	"
Co3	γ-Al$_2$O$_3$	–	67[b]	32	9	41	0.61	[31]
Co4	γ-Al$_2$O$_3$	Re: 0.5 wt%	104[b]	67	20	87	0.84	"
Co5	γ-Al$_2$O$_3$	Re: 0.5 wt%	132[b]	79	30	109	0.83	"
Co6	α-Al$_2$O$_3$	Re: 0.5 wt%	63[b]	63	15	78	1.24	"
Co7	TiO$_2$	–	23[b]	22	8	30	1.30	"
Co8	TiO$_2$	Re: 0.5 wt%	24[b]	20	8	28	1.17	"
Co9	SiO$_2$	–	54[b]	31	10	41	0.76	"
Co10	SiO$_2$	Re: 0.5 wt%	59[b]	38	11	49	0.91	"
Co11	SiO$_2$	La/Co = 0 (atomic ratio)	225[c]	38	233	271	1.20	[1]
Co12	SiO$_2$	La/Co = 0.1	361[c]	292	119	411	1.14	"
Co13	SiO$_2$	La/Co = 0.3	450[c]	253	154	407	0.90	"
Co14	SiO$_2$	La/Co = 0.75	482[c]	214	153	367	0.76	"
Co15	γ-Al$_2$O$_3$	Ru: 0.5 wt%	330[c]	254	53	307	0.93	[2]
Co16	γ-Al$_2$O$_3$	Ru: 0.5 wt%	242[c]	227	41	268	1.11	"
Co17	γ-Al$_2$O$_3$	Ru: 0.5 wt%	176[c]	163	34	197	1.12	"
Co18	MCM-41	Ru: 0.5 wt%	49[a]	55	12	67	1.36	[36]
Co19	MCM-41	Ru: 0.5 wt%	55[a]	57	31	88	1.60	"
Co20	MCM-41	Ru: 0.5 wt%	59[a]	67	41	108	1.83	"
Co21	MCM-41	Ru: 0.5 wt%	116[a]	60	34	94	0.81	"
Co22	SiO$_2$	Ru: 0.5 wt%	93[a]	56	15	71	0.76	"
Co23	SiO$_2$	Ru: 0.5 wt%	36[a]	40	5	45	1.25	[5]
Co24	TiO$_2$	Ru: 0.18 wt%	61.8[a]	40	12	52	0.84	[26]
Co25	SiO$_2$	–	109[a]	60	18.5	78.5	0.72	[27]
Co26	γ-Al$_2$O$_3$	–	95[d]	49.2	10.4	59.6	0.63	[28]
Co27	γ-Al$_2$O$_3$	Ru: 0.5 wt%	285[d]	167	38	205	0.72	"

[a] Based on H$_2$ chemisorption at 100 °C. Max error = ± 5%.
[b] Based on H$_2$ chemisorption at 40 °C. Max error = ± 5%.
[c] Based on H$_2$ chemisorption at 40 °C. Max error = ± 10%.
[d] Based on H$_2$ chemisorption at ambient temperature. Max error = ± 10%.
[e] $N_T^* = N_{CO}^* + N_M^*$. N_{CO}^* and N_M^* were the concentrations of adsorbed CO and surface intermediates, respectively, measured by SSITKA.

Table 4
Chemisorption and SSITKA (methanation) results for Fe catalysts.

Technique		Static chemisorption	Static chemisorption	SSITKA	N_T^*/N_{chem} ($N_{chem} = N_H$ or N_{CO})	Reference
Catalyst samples	Additive[c]	N_H (μmol H/g cat.)	N_{CO} (μmol CO/g cat.)	N_T^* (μmol/g cat.)		
Fe1	Cu: 5; K: 4.2	41.2[d]	–	2.0[g]	0.05	[33]
Fe1	Cu: 5; K: 4.2	4.5[d]	–	1.3[g]	0.29	"
Fe2	–	–	119[e]	25[h]	0.21	[4]
Fe3	Cr: 5	–	232[e]	35[h]	0.15	"
Fe4	Mn: 20	–	140[e]	35[h]	0.25	"
Fe5	Zr: 10	–	191[e]	35[h]	0.18	"
Fe6	K/Fe = 0.015	–	91[e]	40[h]	0.44	[3]
Fe7	Mn/Fe = 0.20	–	141[e]	33[h]	0.23	"
Fe8	Mn/Fe = 0.20	–	108[e]	93[h]	0.86	"
Fe9[a]	K/FeMn = 4	–	63[f]	9	0.14	[32]
Fe9[b]	–	–	63[f]	11	0.17	"

[a] Reaction temperature: 280 °C.
[b] Reaction temperature: 265 °C.
[c] The additive of Fe1 and Fe3–Fe5 was listed based on wt%. The additive of Fe6–Fe9 was listed based on atomic ratio.
[d] Based on H$_2$ chemisorption at 35 °C. Max error = ± 5%.
[e] Based on CO chemisorption at 35 °C. Max error = ± 5%.
[f] Based on CO chemisorption at −196 °C. Max error = ± 5%.
[g] N_{CO}^* was not available in this paper for Fe1, so $N_T^* = N_M^*$ only.
[h] $N_T^* = N_{CO}^* + N_M^*$.

spillover onto Cu which can occur during chemisorption at room temperature and thus affect the results. N_M^* was relatively constant for different H$_2$/CO ratios. The results suggest that the surface carbon intermediate coverage is largely independent of H$_2$ partial pressure in this temperature range. SSITKA results showed that N_{CO}^* went through a maximum with moderate Cu/Ru loading (i.e., moderate Cu coverage). This may be explained by a change in Ru surface structure as a result of Cu decoration. A larger N_T^*/N_{chem} ratio (>2) for Cu-decorated compared with Cu-free Ru catalysts can be observed in Table 5. This probably was due to the Ru surface being blocked by

Cu adatoms. While the amount of chemisorption measured by both techniques decreased accordingly, the effect appeared to be less significant at reaction temperature, probably due to some spillover onto the Cu surface atoms.

Based on the limited number of Ru catalysts studied, there appears to be some possibility to use SSITKA chemisorption measurements at reaction temperature for characterization provided (1) a stoichiometry of $N_T^*/N_{metal,s} = 2$ (since $N_H/N_{metal,s} = 1$ for Ru) and (2) no second inactive component (like Cu) is present that can receive spillover species.

Table 5
Chemisorption and SSITKA (methanation) results for Ru/SiO$_2$ catalysts.

Catalyst samples	Cu/Ru ratio (atomic ratio)	T_{chem}[a] (°C)	N_{chem} (µmol H/ g cat.)	T_{rxn}[b] (°C)	P_{H2}[b,c] (bar)	N_{CO}^*(µmol/g cat.)	N_M^*(µmol/gcat.)	N_T^* [g] (µmol/ g cat.)	N_T^*/N_{chem}	Reference
Ru1	0	25	110[d]	240	0.18	237	4.4	241	2.19	[11]
Ru1	0	25	110[d]	250	0.18	217	5.0	222	2.02	"
Ru1	0	25	110[d]	260	0.18	227	3.8	231	2.10	"
Ru1	0	25	110[d]	270	0.18	202	4.8	207	1.88	"
Ru1	0	25	110[d]	240	0.72	202	5.3	207	1.88	"
Ru1	0	25	110[d]	250	0.72	189	8.3	197	1.79	"
Ru1	0	25	110[d]	260	0.72	194	11.2	205	1.87	"
Ru1	0	25	110[d]	270	0.72	180	13.8	194	1.76	"
Ru1	0	25	110[d]	270[f]	0.45	205	11.6	217	1.97	"
Ru1	0	25	110[d]	270[f]	0.45	184	9.8	194	1.76	"
Ru1	0	25	110[d]	270[f]	0.45	195	8.9	204	1.85	"
Ru1	0	25	110[d]	270[f]	0.45	189	9.0	198	1.80	"
Ru1	0	−196	112.8[e]	240	0.18	241	7.9	249	2.21	[34]
Ru1	0	−196	112.8[e]	240	0.37	207	7.7	215	1.90	"
Ru1	0	−196	112.8[e]	240	0.55	183	9.8	193	1.71	"
Ru2	0.05	−196	96.4[e]	240	0.18	260	8.4	268	2.78	"
Ru3	0.10	−196	60.4[e]	240	0.18	293	7.8	301	4.98	"
Ru4	0.20	−196	39.0[e]	240	0.18	238	5.9	244	6.25	"
Ru5	0.50	−196	23.0[e]	240	0.18	198	3.6	202	8.77	"
Ru2	0.05	−196	96.4[e]	240	0.37	239	9.6	249	2.56	"
Ru3	0.10	−196	60.4[e]	240	0.37	245	7.2	252	4.18	"
Ru4	0.20	−196	39.0[e]	240	0.37	224	6.9	231	5.92	"
Ru5	0.50	−196	23.0[e]	240	0.37	198	3.8	202	8.77	"
Ru2	0.05	−196	96.4[e]	240	0.55	228	10.6	239	2.48	"
Ru3	0.10	−196	60.4[e]	240	0.55	250	8.5	259	4.28	"
Ru4	0.20	−196	39.0[e]	240	0.55	169	5.5	175	4.47	"
Ru5	0.50	−196	23.0[e]	240	0.55	188	2.4	190	8.28	"

[a] At chemisorption conditions.
[b] At reaction conditions.
[c] P_{CO} was fixed at 0.036 bar.
[d] Based on H$_2$ chemisorption at room temperature. Max error = ±5%.
[e] Based on H$_2$ chemisorption at −196 °C. Max error = ±5%.
[f] The results at 270 °C were obtained TOS (5, 25, 50, 77 min).
[g] $N_T^* = N_{CO}^* + N_M^*$.

3.5. Pt catalysts

Table 6 shows that N_T^*/N_{chem} ratios for unpromoted and K$^+$-promoted Pt catalysts were less than 1 regardless whether the support used was SiO$_2$ or C [12,35]. Catalysts containing K$^+$ would be expected to have some of their Pt surface atoms blocked by the promoter for both chemisorbing H$_2$/CO and reaction intermediates. Therefore, this is probably not the cause for the low N_T^*/N_{chem} ratios. Rather, it is likely that lower values of N_T^* at the very high reaction temperature (392 °C) required for methanation on Pt due to lower coverage caused the N_T^*/N_{chem} ratio to be significantly < 1.

3.6. Rh catalysts

Rh/SiO$_2$ catalysts with and without V addition (Rh1 and Rh2) were investigated under methanation conditions by SSITKA [13].

It can be seen from Table 7 that the N_T^*/N_{chem} ratio was almost unity without V promotion (Rh1). However, with the addition of V (Rh2), the high values of N_T^*/N_{chem} (8–24.5) were due to the low H$_2$ chemisorption uptake at chemisorption conditions. The H$_2$ chemisorption results show clearly that H$_2$ adsorption was seriously suppressed at room temperature with the addition of V as has been shown [13,61]. For Rh/V/SiO$_2$ (Rh2), N_M^* and N_{CO}^* decreased as the reduction temperature increased, suggesting that the Rh surface was partially covered by VO$_x$ species, which has been suggested to be a possible cause also for H$_2$ chemisorption suppression.

Investigations of Rh/Al$_2$O$_3$ (Rh3) and Rh/MgO (Rh4) have also been carried out under methanation conditions by Efstathiou and Bennett [37,38] and Efstathiou [39]. Rh4 had values of N_T^*/N_{chem} similar to that for Rh/SiO$_2$ (Rh1), 1.1–1.2 compared to 1.0–1.1, respectively. Although Rh/Al$_2$O$_3$ (Rh3) had values of N_T^*/N_{chem} somewhat smaller than those of Rh/SiO$_2$ (Rh1) and Rh/MgO

Table 6
Chemisorption and SSITKA (methanation) results for Pt catalysts.

Catalyst samples	K$^+$/Pt (atomic ratio)	Support	TOS (min)	N_{chem} (µmol/ g cat.)	N_{CO}^* [c] (µmol/ g cat.)	N_M^* [c] (µmol/ g cat.)	N_T^* [c] (µmol/ g cat.)	N_T^*/N_{chem}	Reference
Pt1	0.1	SiO$_2$	5	55.4[a]	20	0.5	20.5	0.37	[35]
	"	"	90	55.4[a]	20	0.22	20.2	0.36	"
Pt2	0.2	SiO$_2$	5	55.4[a]	16	0.38	16.4	0.30	"
	"	"	90	55.4[a]	16	0.14	16.1	0.29	"
Pt3	0	C	5	278[b]	30	0.37	30.4	0.11	[12]
Pt4	0.2	C	5	264[b]	29	0.31	29.3	0.11	"
Pt5	0.4	C	5	252[b]	30	0.25	30.3	0.12	"
Pt6	0.8	C	5	177[b]	32	0.20	32.2	0.18	"

[a] Based on CO chemisorption at room temperature, in µmol CO/g cat. Max error = ±5%.
[b] Based on H$_2$ chemisorption at 35 °C, in µmol H/g cat. Max error = ±5%.
[c] $N_T^* = N_{CO}^* + N_M^*$.

Table 7
Chemisorption and SSITKA (methanation) results for Rh catalysts.

Catalysts	Promoter	Support	Reduction Temp. (°C)	N_{chem}[a] (μmol H/ g cat.)	Reaction Temp. (°C)	N_{CO}^* [b] (μmol/ g cat.)	N_M^* (μmol/ g cat.)	N_T^* [c] (μmol/ g cat.)	N_T^*/N_{chem}	Ref.
Rh1	–	SiO$_2$	300	31.1	280	31.2	0.39	31.6	1.0	[13]
	"	"	600	31.1	280	32.6	0.38	32.9	1.1	"
Rh2	V: 1.5 wt%	SiO$_2$	300	1.2	280	18.5	0.25	18.8	15.6	"
	"	"	400	0.6	280	14.5	0.17	14.7	24.5	"
	"	"	500	0.4	280	9.0	0.07	9.1	22.7	"
	"	"	600	0.3	280	2.3	0.01	2.3	7.7	"
Rh3	–	γ-Al$_2$O$_3$	350	60	220	36.6	2.4	39.0	0.65	[37,38]
	"	"	350	60	260	29.4	3.24	32.6	0.54	"
Rh4	–	MgO	350	30	260	32.1	0.18	32.3	1.08	[39]
	"	"	350	30	300	34.8	0.30	35.1	1.17	"

[a] Based on H$_2$ chemisorption at 35 °C (Rh1 and Rh2) or 25 °C (Rh3 and Rh4). Max. error = ±5%.
[b] The data in Ref. [13] were corrected by multiplying by 2 due to a calculation mistake made in the original paper.
[c] $N_T^* = N_{CO}^* + N_M^*$.

Table 8
Hypothetical Co average particle size results from different characterization techniques.

Technique	TEM	Static chemisorption	SSITKA	Probable conclusions
Case (a)	Small	Small	Small	Confirmation
Case (b)	Small	Small	Large	Low θ at reaction conditions due to surface blockage by coking/poisons or due to adsorption equilibrium at higher temperature
Case (c)	Small	Large	Small	"Suppression" of chemisorption at 25–100 °C due to slow kinetics
Case (d)	Large	Small	Small	Incorrect interpretations of TEM results are due to clustering of small metal particles or overlapping of a lot of particles in 3D that may appear as large particles in 2D
Case (e)	Small	Large	Large	Metal particles are small, but a lot of chemisorption blocked by support or promoter species decoration
Case (f)	Large	Small	Large	Overestimation of metal dispersion due to hydrogen spillover during static chemisorption
Case (g)	Large	Large	Large	Confirmation

(Rh4), all of these non-promoted Rh catalysts had values in the range of ca. 0.6–1.2. It is possible that some of the differences in the ratios for Rh/Al$_2$O$_3$ (Rh3) were either due to (1) differences in the isotopic tracing procedures used and/or (2) a partial blockage of some Rh sites by additional spectator surface molecules (such as formates) formed on the acid sites of alumina.

Based on the limited Rh data available, there does appear to be a possibility to characterize simple Rh catalysts such as Rh on a non-SMSI-inducing support like SiO$_2$, Al$_2$O$_3$, and MgO using SSITKA chemisorption results (with $N_T^*/N_{metal,s} = 1$). However, one would need to be careful when promoters or strong support interactions are present.

4. Conclusions

The relationships of the total amounts of chemisorbed species on Group VIII metal catalysts at reaction temperature {measured during CO hydrogenation by SSITKA (N_T^*)} and at 25–100 °C {measured by static H$_2$ or CO chemisorption (N_{chem})} were systematically presented in this paper for Co, Fe, Pt, Ru, and Rh. Ideally, the ratio of N_T^*/N_{chem} should be close to unity if there is full coverage of the metal surface at both static chemisorption and reaction temperatures. However, N_T^*/N_{chem} can deviate from unity due to H$_2$ spillover, carbon deposition, formation of metal carbides, SMSI, or other mechanisms causing active site blockage.

It is concluded based on data that Co catalysts routinely have close-to-unity values for N_T^*/N_{chem} for a wide variety of supports and promoters. Larger N_T^*/N_{chem} ratios, however, are typical for Ru catalysts, even when supported on SiO$_2$ without promoters. N_T^*/N_{chem} ratios close to one were observed for Rh/SiO$_2$ and Rh/MgO, but V promotion on Rh/ SiO$_2$ increased this significantly be-

cause of H$_2$ chemisorption suppression during static chemisorption. Values much smaller than unity can be observed for both Fe and Pt catalysts. Site blockage by carbon deposition at reaction temperatures may be a possible explanation for low N_T^*/N_{chem} values observed for Fe-based catalysts. The low values of N_T^*/N_{chem} (due to low N_T^*) for Pt catalysts are probably due to the lower coverage at the high reaction temperature (392 °C), necessary for methanation on Pt. Thus, Co is the best candidate for using chemisorption measured at reaction temperature by SSITKA for characterization. Both Ru and Rh look also like possibilities, provided care is taken to avoid catalysts containing certain components, and, in the case of Ru, a stoichiometry of $N_T^*/N_{metal,s} = 2$ is used.

It has been stated that static chemisorption measurements at standard temperatures (25–100 °C) may not be representative of real active site concentrations under reaction conditions [18,29]. SSITKA has been shown to measure such concentrations. However, it can also provide an alternative means for better understanding causes of chemisorption disruption at even static chemisorption conditions. For Co catalysts, especially, SSITKA can be applied as a complementary technique to static chemisorption, XRD line broadening, and TEM for better characterizing metal dispersion (availability of surface metal atoms) and metal particle size. Table 8 gives a comparison for hypothetical particle size measurements based on TEM, static chemisorption, and SSITKA results for the same samples. When the results are consistent {(a) and (g)}, SSITKA results just confirm the other measurements. However, when the results are inconsistent with each other, SSITKA results provide a means to better ascertain the cause for the inconsistency. However, currently, such an application is limited to Co catalysts. More data are required for the other metals addressed, before SSITKA can be used with confidence for metal dispersion characterization.

Acknowledgment

References

[1] G.J. Haddad, B. Chen, J.G. Goodwin Jr., J. Catal. 161 (1996) 274.
[2] A.R. Belambe, R. Oukaci, J.G. Goodwin Jr., J. Catal. 166 (1997) 8.
[3] N. Lohitharn, J.G. Goodwin Jr., J. Catal. 260 (2008) 7.
[4] N. Lohitharn, J.G. Goodwin Jr., J. Catal. 257 (2008) 142.
[5] J. Panpranot, J.G. Goodwin Jr., A. Sayari, J. Catal. 213 (2003) 78.
[6] M. Agnelli, H.M. Swaan, C. Marquez-Alvarez, G.A. Martin, C. Mirodatos, J. Catal. 175 (1998) 117.
[7] M.A. Vannice, R.L. Garten, J. Catal. 56 (1979) 236.
[8] C.H. Bartholomew, R.B. Pannell, J.L. Butler, J. Catal. 65 (1980) 335.
[9] S.J. Tauster, S.C. Fung, R.L. Garten, J. Am. Chem. Soc. 100 (1978) 170.
[10] R.C. Reuel, C.H. Bartholomew, J. Catal. 85 (1984) 63.
[11] I.-G. Bajusz, J.G. Goodwin Jr., J. Catal. 169 (1997) 157.
[12] J.Z. Zhang, Y.-T. Tsai, K.L. Sangkaewwattana, J.G. Goodwin Jr., J. Catal. 280 (2011) 89.
[13] J. Gao, X. Mo, J.G. Goodwin Jr., Catal. Today 160 (2011) 44.
[14] J. Happel, Chem. Eng. Sci. 33 (1978) 1567.
[15] C.O. Bennett, ACS Symp. Ser. 178 (1982) 1.
[16] P. Biloen, J. Mol. Catal. 21 (1983) 17.
[17] M. Depontes, G.H. Yokomizo, A.T. Bell, J. Catal. 104 (1987) 147.
[18] J.G. Goodwin Jr., S. Kim, W.D. Rhodes, Catalysis 17 (2003) 320.
[19] D.M. Stockwell, J.S. Chung, C.O. Bennett, J. Catal. 112 (1988) 135.
[20] P. Biloen, J.N. Helle, F.G.A. van den Berg, W.M.H. Sachtler, J. Catal. 81 (1983) 450.
[21] D.M. Stockwell, C.O. Bennett, J. Catal. 110 (1988) 354.
[22] M. de Pontes, G.H. Yokomizo, A.T. Bell, J. Catal. 104 (1987) 147.
[23] F. Rohr, O.A. Lindvåg, A. Holmen, E.A. Blekkan, Catal. Today 58 (2000) 247.
[24] K.R. Krishna, A.T. Bell, J. Catal. 130 (1991) 597.
[25] J. Barrault, A. Alouche, Appl. Catal. 58 (1990) 255.
[26] H.A.J. van Dijk, The Fischer–Tropsch synthesis: a mechanistic study using transient isotopic tracing, Ph.D. dissertation (Eindhoven University Press, Eindhoven, 2001).
[27] C.A. Mims, L.E. McCandlish, J. Phys. Chem. 91 (1987) 929.
[28] A. Kogelbauer, J.G. Goodwin Jr., R. Oukaci, J. Catal. 160 (1996) 125.
[29] S.L. Shannon, J.G. Goodwin Jr., Chem. Rev. 95 (1995) 677.
[30] B. Jongsomjit, J. Panpranot, J.G. Goodwin Jr., J. Catal. 215 (2003) 66.
[31] V. Frøseth, S. Storsæter, Ø. Borg, E.A. Blekkan, M. Rønning, A. Holmen, Appl. Catal. A – Gen. 289 (2005) 10.
[32] D.M. Stockwell, D. Bianchi, C.O. Bennett, J. Catal. 113 (1988) 13.
[33] K. Sudsakorn, J.G. Goodwin Jr., A.A. Adeyiga, J. Catal. 213 (2003) 204.
[34] B. Chen, J.G. Goodwin Jr., J. Catal. 158 (1996) 511.
[35] I.-G. Bajusz, D.J. Kwik, J.G. Goodwin Jr., Catal. Lett. 48 (1997) 151.
[36] J. Panpranot, J.G. Goodwin Jr., A. Sayari, J. Catal. 211 (2002) 530.
[37] A.M. Efstathiou, C.O. Bennett, J. Catal. 120 (1989) 118.
[38] A.M. Efstathiou, C.O. Bennett, J. Catal. 120 (1989) 137.
[39] A.M. Efstathiou, J. Mol. Catal. 67 (1991) 229.
[40] A.M. Efstathiou, X.E. Verykios, Appl. Catal. A – Gen. 151 (1997) 109.
[41] A.Y. Khodakov, B. Peregryn, A.S. Lermontov, J.-S. Girardon, S. Pietrzyk, Catal. Today 106 (2005) 132.
[42] P. Winslow, A.T. Bell, J. Catal. 94 (1985) 385.
[43] J.M. Zowtiak, C.H. Bartholomew, J. Catal. 83 (1983) 107.
[44] S.J. Tauster, S.C. Fung, J. Catal. 55 (1978) 29.
[45] R.T.K. Baker, S.J. Tauster, J.A. Dumesic (Eds.), Strong Metal–Support Interactions, American Chemical Society, Washington, DC, 1986.
[46] C.-M. Lu, Y.-M. Lin, I. Wang, Appl. Catal. A – Gen. 198 (2000) 223.
[47] V.V. Rozanov, O.V. Krylov, Russ. Chem. Rev. 66 (1997) 107.
[48] P.A. Sermon, G.C. Bond, Catal. Rev. 8 (1974) 211.
[49] A.D. Lueking, R.T. Yang, Appl. Catal. A – Gen. 265 (2004) 259.
[50] P. Forzatti, L. Lietti, Catal. Today 52 (1999) 165.
[51] C.H. Bartholomew, Appl. Catal. A – Gen. 212 (2001) 17.
[52] H.M. Swaan, V.C.H. Kroll, G.A. Martin, C. Mirodatos, Catal. Today 21 (1994) 571.
[53] G.-J. Kim, D.-S. Cho, K.-H. Kim, J. Kim, Catal. Lett. 28 (1994) 41.
[54] T. Zhang, M.D. Amiridis, Appl. Catal. A – Gen. 167 (1998) 161.
[55] C.H. Bartholomew, Catal. Rev. – Sci. Eng. 24 (1982) 67.
[56] S.B. Wang, G.Q.M. Lu, J. Chem. Technol. Biotechnol. 75 (2000) 589.
[57] S.H. Ali, J.G. Goodwin Jr., J. Catal. 171 (1997) 333.
[58] S.H. Ali, J.G. Goodwin Jr., J. Catal. 171 (1997) 339.
[59] R. Riva, H. Miessner, R. Vitali, G. Del Piero, Appl. Catal. A – Gen. 196 (2000) 111.
[60] J.W. Niemantsverdriet, A.M. van der Kraan, W.L. van Dijk, H.S. van der Baan, J. Phys. Chem. 84 (1980) 3363.
[61] J. Gao, X. Mo, A.C. Chien, W. Torres, J.G. Goodwin Jr., J. Catal. 262 (2009) 119.